J. COMBIN. MATH. COMBIN. COMPUT. 127a (2025) 4523--4542

Journal of Combinatorial Mathematics
and Combinatorial Computing
www.combinatorialpress.com/jcmcc

Combinatorial Press

A multi-stage dynamic planning-based optimization method for post-disaster resilience enhancement and flexible resource dispatch of distribution networks in coastal cities

Guowei Liu[1], Hao Dai1, Hao Deng[1], Lisheng Xin[1,✉], Longlong Shang[1]

[1] *Distribution Network Management Department, Shenzhen Power Supply Co., Ltd., Shenzhen, Guangdong, 518000, China*

ABSTRACT

The study proposes a multi-stage dynamic resilient recovery strategy based on multiple energy storage to cope with distribution network failures after a disaster in a coastal city, and the post-disaster recovery of the urban distribution network is planned in phases, which is divided into the first stage of emergency response, the second stage of energy storage recovery and the third stage of economic optimization. Then the post-disaster defense measures of the coastal city are improved by optimizing the recovery strategy. After the calculation example design, the post-disaster recovery and resource scheduling effects of this paper's multi-stage dynamic recovery model are examined through simulation experiments. The multi-stage dynamic recovery model of this paper takes 261 minutes to recover the urban distribution network, which is shorter than the 273 minutes of the traditional recovery model, and the post-disaster resilience is improved. The proposed dispatching scheme based on the multi-stage dynamic recovery model in this paper uses only 13 vehicles, which is the least number of vehicles among all dispatching schemes. The traveling path of mobile emergency resources of this paper's scheme is most consistent with the post-disaster restoration scenario. The combined level of load reactive power and active power restoration of this paper's scheme is optimal.

Keywords: Multi-phase dynamic recovery, resilient recovery strategy, post-disaster recovery, resource scheduling

1. Introduction

Coastal cities are often subject to natural disasters such as typhoons and heavy rains due to their geographical location and climatic conditions [1]. These disasters not only bring inconvenience to the life of local residents, but also cause serious damage to the power infrastructure, especially the distribution network, which is prone to blackout accidents [2-4]. Since entering the 21st century, the Southern Power Grid Corporation has paid more attention to the emergency disaster prevention and

✉ Corresponding author.
E-mail address: 19928723443@163.com (L. Xin).
Received 25 February 2024; Revised 05 April 2024; Accepted 15 December 2024; Published Online 15 April 2025.
DOI: 10.61091/jcmcc127a-256

control of distribution networks, requiring focusing on the weak links of distribution, making up the short board of distribution, adjusting according to the local conditions, and accurately remodeling and upgrading [5-7]. China Power Grid in the self-correction process found that the coastal areas of the distribution network base pole emergency disaster-resistant capacity is insufficient, typhoons, heavy rain and other bad weather base pole shaking, skewing, collapse and other situations occur frequently, seriously affecting the quality of electricity customers [8-10].

In response to this situation, distributed power sources in the distribution network and dispatch emergency repairers can be coordinated to repair damaged critical paths to restore important loads, thus reducing losses [11-12]. In this regard, during the dynamic change of the availability of damaged lines, the structure of each island in the distribution network changes accordingly, and each formed electrical island should maintain a radial topology, i.e., a dynamic radial topology. Based on this, post-disaster mobile resource scheduling is synchronized with distribution network load restoration, while the radial structure of the distribution network needs to be ensured [13-16].

At the same time, the post-disaster effective cooperation of recovery resources can realize rapid and stable load recovery, but it is difficult to realize the large-scale efficient transfer of resources under the flooding scenario, and the pre-disaster deployment of recovery resources can improve the system resource layout in advance, but this process needs to take into account the actual deployment of each resource after the disaster [17-19]. Therefore, it is crucial to study the pre-disaster deployment and post-disaster coordinated restoration methods of distribution network restoration resources under wind and flood compound disasters by fully considering the linkage relationship between the pre-disaster and post-disaster phases [20-22].

The article proposes a multi-stage dynamic resilience recovery strategy based on multiple energy storage, which divides urban post-disaster distribution network repair into the first stage of economic response, the second stage of energy storage recovery, and the third stage of economic optimization, and improves the post-disaster resilience of the urban distribution network points through phased planning. Considering the disaster characteristics of coastal cities and taking typhoon as an example, measures to defend coastal cities against typhoon after disaster are proposed through optimization of recovery strategies. After the disaster, the path and time of emergency repair planned by this paper's multi-stage dynamic recovery model are simulated through the analysis of arithmetic examples, and compared with the traditional recovery model to verify the superiority of this paper's model. Finally, the resource scheduling efficiency of the multi-stage dynamic recovery model is examined by simulating the resource mobilization results of each scenario.

2. Multi-stage dynamic planning based distribution network restoration strategy for coastal cities

2.1. Multi-stage dynamic elastic recovery strategy based on multiple energy storage

A multi-stage dynamic resilience recovery strategy for the distribution network considering the integrated electric-gas energy network and transportation network is shown in Fig. 1, where MESS is a movable energy storage system. First, in the first stage of emergency response, the output of gas turbines is increased and network reconfiguration is performed to optimize the operation of the distribution network. Second, in the second stage of energy storage restoration, the MESS further supplies power to the orphaned portion of the island that has lost power based on the first stage. Finally, in the third stage of economic optimization, a mathematical model for economic optimization of distribution network disaster recovery is developed with the objective function of minimizing the total cost of the three resilience recovery measures.

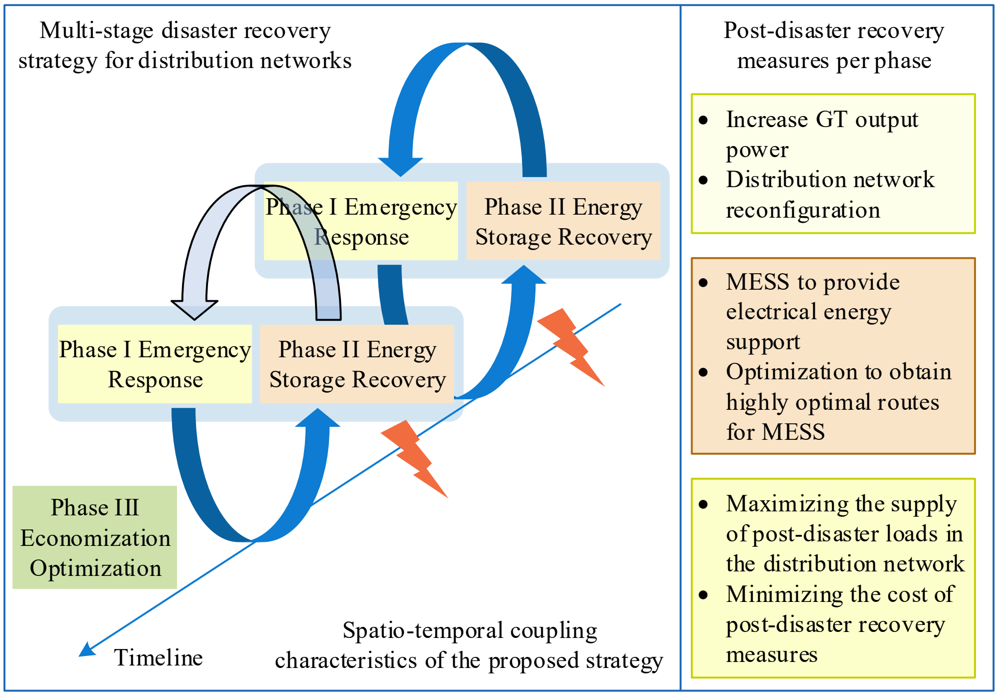

Fig. 1. Post-disaster recovery strategy model proposed in this chapter

2.1.1. Phase I emergency response.In the initial phase of the fault, the natural gas network increases the output through gas turbines, and the distribution network is also reconfigured through the on/off of line switches for network reconfiguration, with an optimization objective function in order to maximize the restoration of power supply to the critical loads, and prioritize the restoration of critical loads with a greater degree of importance in the distribution network. Therefore, a mathematical model of the emergency response in the distribution network in the first stage is developed, which is described as a MILP model [23-24].

The objective function of the emergency response in the distribution network in the first stage is to maximize the restoration of lost power loads in the distribution network and the expression is shown below:

$$\min \sum_{i=1}^{T} \sum_{i=1}^{N} w_t \cdot \left(1-\delta_{i,t}\right) \cdot P_{i,t}^{load} \tag{1}$$

Where, $\delta_{i,t}$ denotes the load restoration degree coefficient of node i at the moment of t, and w_i denotes the load importance degree coefficient of node w_i.

Solve the above MILP model for the first stage emergency response, change the distribution network topology and the coordinated and optimized operation with the natural gas network to achieve the purpose of fast and reliable maximized restoration of power supply to the important loads in the distribution network in the first stage emergency response. Continue to determine the location of the lost load node or the unpowered microgrid formed by the lost load node, and wait for the second stage of energy storage restoration to carry out the next step of restoring power to the lost load node.

2.1.2. Phase II energy storage restoration.After the first stage of emergency response, the supply of gas turbines and the network reconfiguration of the distribution network two kinds of disaster recovery measures have maximized the restoration of power supply to the important loads in the distribution network, the role of the secondary storage mobile restoration of power supply is to restore the existing important loads on the basis of moving the MESS in the distribution network, to play the role of emergency power supply of the MESS in the total degree of the shortest time of the objective function for the The nodes of important loads or general loads that have not been restored to the power supply by the role of the disaster recovery measures in the first stage continue to restore the power supply to the loads, and the second stage of the energy storage restoration process is shown in Fig. 2.

The green part in Fig. 2 is the problem of finding the optimal path for MESS movement in the transportation network. The optimal path Floyd algorithm based on DTA is as follows: first, the CTM-based DTA model is solved to obtain the dynamic traffic network equilibrium. Second, the traveling time on each road in the traffic network, i.e., the time weight matrix, is obtained. Finally, the optimal path and the shortest traveling time of the MESS are obtained by the DTA-based Floyd algorithm [25].

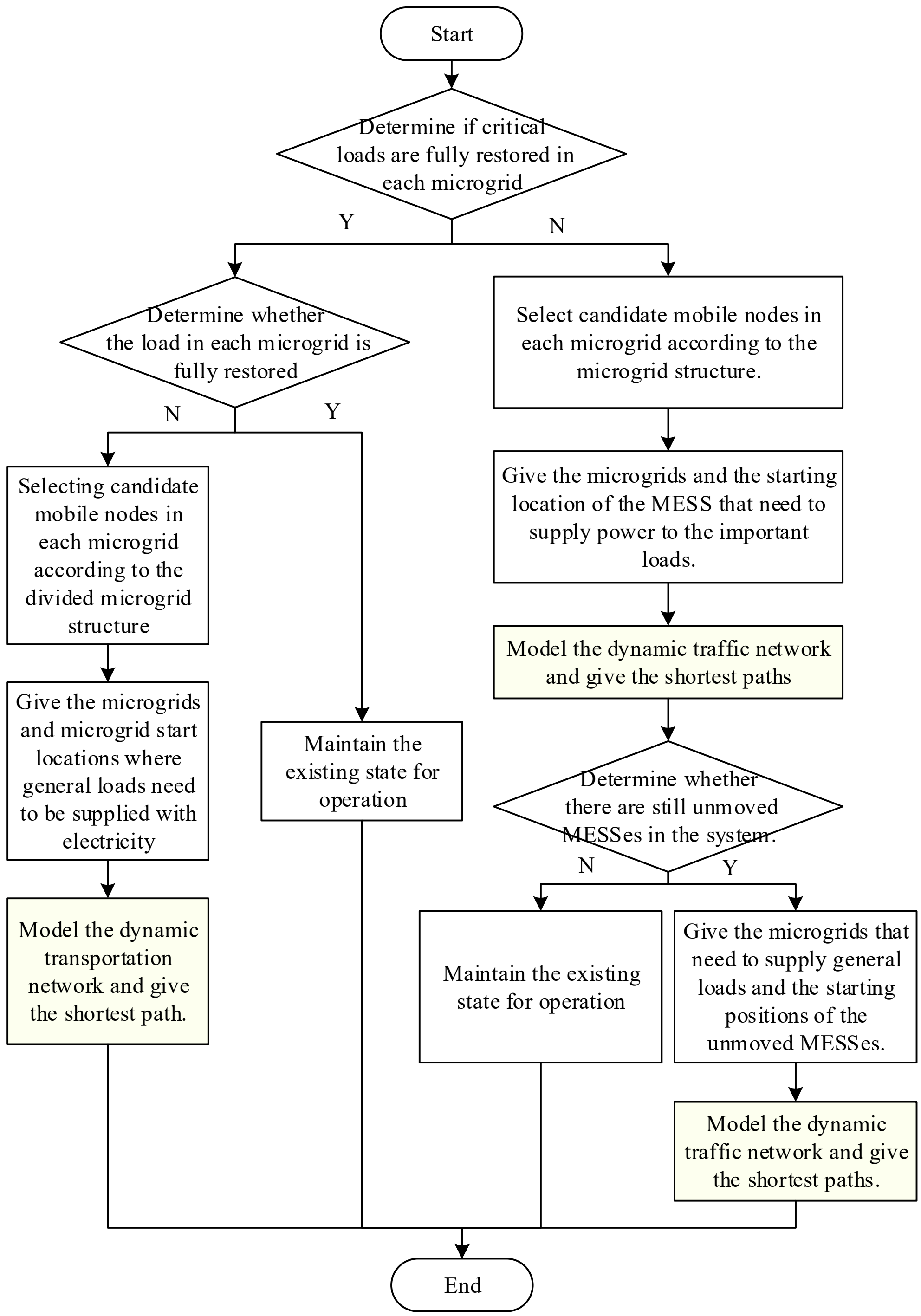

Fig. 2. Second stage of energy storage recovery

2.1.3. Third-stage economic optimization. After the system has gone through the first stage of emergency response and the second stage of energy storage recovery, and after judging that the system will not continue to fail, the system undergoes the third stage of economic optimization. After the MESS is moved to the corresponding location to restore normal power supply, in order to ensure that the system resilience restoration process using a variety of restoration measures can ensure the economic optimization on the basis of restoring power supply to the maximum load, by establishing the cost model of the three optimization measures of interruption of power supply penalty cost, power purchase cost of the substation as well as the cost of network reconfiguration, the cost of natural gas consumed by the gas turbine, and the cost of operation and maintenance of the MESS, through the interruption of supply penalty cost to ensure maximum restoration of supply load, and optimizing and adjusting the gas turbine's output profile, network reconfiguration and MESS's output profile with the optimization objective of the interruption of supply penalty function, the substation's power purchase cost, and the cost and minimum of the three measures. The MILP model for this phase is shown below:

$$\min f = f_1 + f_2 + f_3 + f_4 + f_5 \tag{2}$$

$$f_1 = \sum_{t=1}^{T}\sum_{i=1}^{N}\left[C_i^{load} \cdot \left(P_{i,t}^{lood} - \delta_{i,t} \cdot P_{i,t}^{lood} \right) \right] \tag{3}$$

$$f_2 = \sum_{t=1}^{T}\sum_{i=1}^{N_{GT}}\left(C_t^{GT} \cdot 3600 \cdot M_{m,t}^{GT} \cdot \Delta t \right) \tag{4}$$

$$f_3 = \sum_{t=1}^{T}\sum_{i=1}^{N_{MESS}}\left(C^{MESS}\left(P_{i,t}^{ch} + P_{i,t}^{dis} \right) \cdot \Delta t \right) \tag{5}$$

$$f_4 = \sum_{l=1}^{L}\sum_{t=1}^{T-1} C^{Sitch}\left| S_{l,t+1} - S_{l,z} \right| \tag{6}$$

$$f_5 = \sum_{t=1}^{T} C_t^{E} \cdot P_t^{sub} \tag{7}$$

where C_i^{losd} denotes the penalty cost function for interruption of power supply, C_i^{GT} denotes the price of natural gas consumed by the gas turbine at t the moment of time, C^{MESS} denotes the maintenance cost coefficient of the MESS battery, C^{Sitch} denotes the cost of one switch action, C_t^E denotes the real-time price of electricity purchased from the substation, f denotes the total cost function, f_1 denotes the load penalty cost function for interruption of power supply, f_2 denotes the cost function of gas turbine support of power supply, f_3 denotes the operation and maintenance cost of the MESS, f_4 denotes the cost function of switch action for each reconfiguration of the network, $S_{i,t}$ denotes the line state of the line l at the moment of t time, and f_5 denotes the cost function of electricity purchased from the substation in the distribution network.

In the third-stage economic optimization model, Eq. (3) represents the penalty cost function for interruption of power supply, Eq. (4) represents the cost function for gas turbine consumption of natural gas, Eq. (5) represents the MESS maintenance cost function, Eq. (6) represents the cost function for the number of switching times for network reconfiguration, and Eq. (7) represents the cost function for the purchase of power from the substation. By minimizing the cost of various measures in the objective function, multiple resilience restoration measures are coordinated and optimized on the basis of guaranteeing the restoration of power supply.

After solving the third stage economic optimization model, there will be possible results: one is that the amount of electricity in the system is sufficient to support the restoration of power supply to all loads in the distribution network. The other is that there are still loads in the system that have not been restored to power after the three phases of restoration, at which point the system sends a command to its superiors to wait for the next resilient restoration phase to carry out the maintenance and restoration of power phase.

2.2. Post-disaster typhoon defense measures considering recovery strategy optimization

Because the research object of this paper is a coastal city, the type of disaster with the highest frequency is typhoon, so the author takes typhoon disaster as the entry point to study the optimization strategy of post-disaster distribution network restoration in coastal cities.

In the practice of the power supply bureau to cope with typhoon disasters, the urban distribution network defense measures based on rapidity enhancement mainly include: improving and perfecting the fault site control mechanism, establishing the command center command system, optimizing the fault repair strategy, increasing the application of non-stop operation technology in the fault outage, and perfecting the remote control operation and test delivery strategy. This section mainly discusses the impact of optimizing fault repair strategies on the resilience of urban distribution networks after the typhoon makes landfall.

Optimizing the fault repair strategy after typhoon landfall can be modeled as a mixed-integer linear programming problem, according to the distance from the repair team's residence to the damaged power facilities and the limited repair resources, considering the distributed power supply in the distribution network, the reconfiguration of the network frame after the transfer of power supply to the distribution network after the disaster and the path of the repair team to participate in the emergency repair, the optimal scheduling of repair, which determines the optimal path of the repair team to participate in the repair work. Optimal path. The optimization objective function consists of two parts, i.e., to prioritize the restoration of the more important loads with higher loads and to make the equipment repair time the shortest, as shown below:

$$\max_{\Gamma,Y} \gamma_1 \sum_{\forall t} \sum_{\forall i} {\eta_i}^D \kappa_{i,} p_{i,t}^D - \gamma_2 \sum_{\forall t} \sum_{\forall m} B_m t h_{m,t} \tag{8}$$

where γ is the component weight, η_i denotes the priority weight of the load supplied by the distribution line, $\kappa_{i,t}$ denotes a binary variable for whether the load supplied by the power equipment can be restored to normal power supply after the failure of the power equipment, B_m denotes a constant for whether the damaged power equipment is an electricity-related public safety hazard, and $h_{m,t}$ denotes a binary variable for when the damaged power equipment will be repaired.

The constraints satisfied by this objective function are as follows:

1) Trend-related constraints: first, the positive direction of each distribution line is set, the parent and child nodes correspond to the nodes in the direction of inflow and outflow of the trend, respectively, and the value is negative when the actual power flow direction is opposite to the set positive direction. The AC current operation constraints are as follows:

$$\sum_{\forall k \in K} P_{k,t} + p_{k,s}^{DG} = \sum_{\forall k \in K} P_{k,t} + \kappa_{k,s} p_{k,t}^{D}, \forall i, \forall t \tag{9}$$

$$\sum_{\forall k \in K} Q_{k,t} + q_{k,t}^{DG} = \sum_{\forall k \in K} Q_{k,t} + \kappa_{k,t} q_{k,t}^{D}, \forall i, \forall t \tag{10}$$

$$V_{j,t} - V_{i,t} + \frac{R_k P_{k,t} + X_k Q_{k,t}}{V_{i,t}} \le \left(1 - u_{k,t}^L\right) M, \forall k, \forall t \tag{11}$$

$$-\left(1 - u_{i,}^L\right) M \le V_{j,t} - V_{i,t} + \frac{R_k P_{k,t} + X_k Q_{k,t}}{V_{i,t}}, \forall k, \forall t \tag{12}$$

$$1 - \varepsilon \le V_{i,t} \le 1 + \varepsilon, \forall i, \forall t \tag{13}$$

$$\kappa_{i,t+1} \geq \kappa_{i,t}, \forall i, \forall t \tag{14}$$

where $u_{k,t}^{L}$ is a binary variable that represents the coefficient of the power of the distribution line after the typhoon has made landfall, which takes the value of 0 when the line is damaged and is out of service, and the value of 1 when the line is in normal operation.

2) Distributed power constraints for urban distribution networks:

$$0 \leq P_{i,t}^{DG} \leq P_{i}^{DG\max} U_{i,t}^{G}, \forall i, \forall t \tag{15}$$

$$0 \leq Q_{i,t}^{DG} \leq Q_{i}^{DG\max} U_{i,t}^{G}, \forall i, \forall t \tag{16}$$

3) Power constraints on urban distribution network lines after typhoon landfall:

$$-u_{k,t}^{L} P_{k}^{\max} \leq P_{k,t} \leq u_{k,t}^{L} P_{k}^{\max}, \forall k, \forall t \tag{17}$$

$$-u_{k,t}^{L} Q_{k}^{\max} \leq Q_{k,t} \leq u_{k,t}^{L} Q_{k}^{\max}, \forall k, \forall t \tag{18}$$

4) After the typhoon makes landfall, the line trips due to faults to interrupt the load power supply, the distributed power sources in the urban distribution network will supply power to some of the loads, forming an islanded microgrid, and the following constraints are used to ensure a radial urban distribution network structure:

$$\beta_{i,j,t} + \beta_{j,i,t} = u_{k,t}^{L}, \forall k, \forall t \tag{19}$$

$$\beta_{i,j,t} = 0, \forall i, j \in BS, \forall t \tag{20}$$

$$\sum_{\forall i} \beta_{i,j,t} \leq 1, \forall j, \forall t \tag{21}$$

5) There are S_{σ} repair teams in a repair site σ, the repair teams are numbered as c, the set of all repair teams in σ is denoted as C, and the set of damaged distribution equipment is denoted as N. $x_{m,n,C}^{\sigma}$ is introduced to denote the binary variable of the repair team c passing through the faulty element m and traveling to the faulty element n in repair site σ, and $y_{m,c}^{\sigma}$ denotes the binary variable of the repair team c traveling to the faulty element m in repair site σ. First of all, after the repair team arrives at the faulty element and repairs the faulty equipment, it needs to leave the repair area immediately to the next area to repair the next damaged distribution equipment, and constructs the constraints as follows:

$$\sum_{\forall n \in N \setminus \{m\}} \left(x_{m,n}^{\sigma} - x_{n,m,c}^{\sigma} \right) = 0, \forall \sigma, \forall m \in N, \forall c \in C \tag{22}$$

where $N \setminus \{m\}$ is the set in set N excluding set $\{m\}$. In addition, Eq. (23) indicates that all the repair teams depart from the repair site to the faulty node, (24) indicates that all the teams involved in the fault repair work return to the repair site after completing the repair task, and (25) indicates that each faulty element is repaired by only one set of fault repairers for the element:

$$\sum_{\forall m \in N} x_{0,m,c}^{\sigma} = 1, \forall \sigma, \forall c \in C \tag{23}$$

$$\sum_{\forall c \in C} \sum_{\forall m \in N} x_{m,0,c}^{\sigma} = S_{\sigma}, \forall \sigma \tag{24}$$

$$\sum_{\forall \sigma} \sum_{\forall c \in C} y_{m,c}^{\sigma} = 1, \forall m \in N \tag{25}$$

6) In order to ensure that personnel involved in fault repair do not travel to distribution network equipment where fault repair cannot be completed at this stage, the following constraints are established:

$$y_{m,c}^{\sigma} = \sum_{\forall n \in N \setminus \{m\}} x_{m,n,c}^{\sigma}, \forall \sigma, \forall c \in C, \forall m \in N \tag{26}$$

$$y_{m,c}^{\sigma} = 0, \forall \sigma, \forall m \in U_c, \forall c \in C \tag{27}$$

7) When the repair team arrives at the damaged distribution equipment that it is scheduled to repair, it will use the time of $\tau_{m,c}^{\sigma}$ to complete the repair of that damaged distribution equipment and arrive at the next area to carry out the repair of the next damaged distribution equipment after $\hat{\tau}_{m,n}^{\sigma}$. The following constraints can be established regarding the repair time of the faulty components:

$$\begin{aligned} & t_{m,c}^{\sigma} - t_{n,c}^{\sigma} + t_{m,c}^{\sigma} + \hat{t}_{m,n,c}^{\sigma} \le M\left(1 - x_{m,n,c}^{\sigma}\right) \\ & \forall \sigma, \forall m \in N, \forall n \in N, \forall c \in C \end{aligned} \tag{28}$$

$$0 \le t_{m,c}^{\sigma} \le M y_{m,c}^{\sigma}, \forall \sigma, \forall m \in N, \forall c \in C \tag{29}$$

$$y_{m,n}^{\sigma} = 0, \forall \sigma, \forall m \in U_c, \forall n \in N \tag{30}$$

$$\begin{aligned} & \sum_{\forall c \in C} \left(t_{m,c}^{\sigma} + \tau_{m,x}^{\sigma} y_{m,c}^{\sigma}\right) \le \sum_{\forall t} t \cdot f_{m,s}^{\sigma} \\ & \le \sum_{\forall c \in C} \left(t_{m,c}^{\sigma} + \tau_{m,c}^{\sigma} y_{m,c}^{\sigma}\right) + 1 - \varepsilon, \forall \sigma, \forall m \in N \end{aligned} \tag{31}$$

where M is a positive number with sufficiently large value and ε is an arbitrarily small real number.

(8) When the repair crew completes the repair of the damaged distribution network equipment components, the equipment will be put into the grid use according to the relevant protocols, which should satisfy the following constraints:

$$z_{m,t}^{\sigma} \le \sum_{r=1}^{t-1} f_{m,r}^{\sigma}, \forall \sigma, \forall m \in N, \forall t \tag{32}$$

$$u_{m,t}^{L} \le z_{m,t}, \forall \sigma, \forall m \in N, \forall t \tag{33}$$

3. Analysis of examples

In this chapter, the improved IEEE 33-node active distribution network is used as an example, and the example is set up with 5 remote control switches and 9 manual switches, which are located as shown in Fig. 3. The important nodes are 17, 21, 24, and 31.The setup grid contains 2 maintenance sites, 2 line maintenance teams, and 2 switch operation teams. Line maintenance team 1 and switch operation team 1 belong to maintenance site 1, and line maintenance team 2 and switch operation team 2 belong to maintenance site 2.

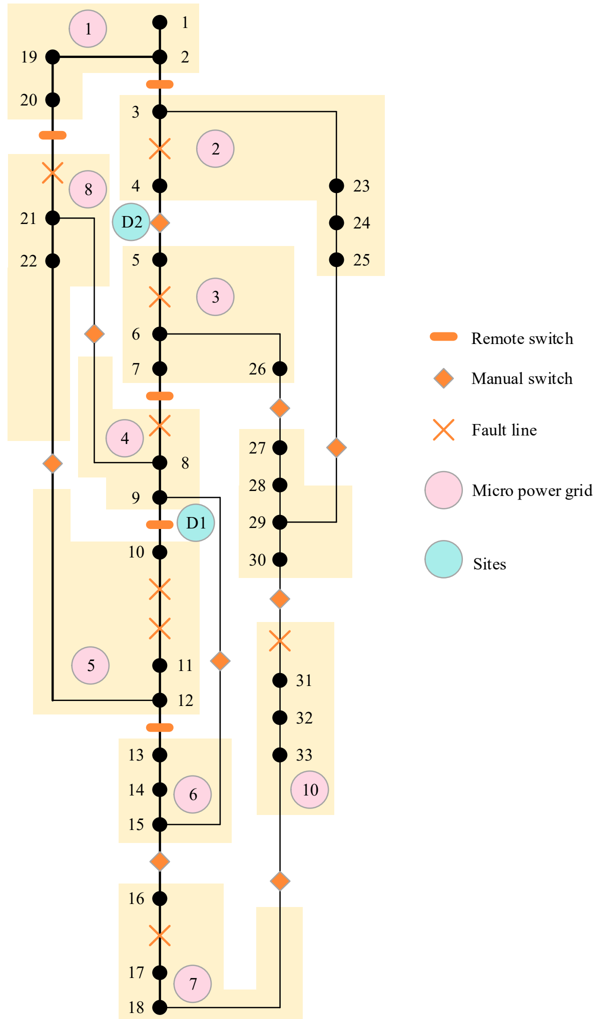

Fig. 3. IEEE33 node system

3.1. Analysis of post-disaster recovery effects

3.1.1. Simulation results.Using the multi-stage dynamic resilient recovery model in this paper to solve the algorithm, the scheduling paths and times for the maintenance team and the development team and are shown in Table 1. According to Table 1, it can be seen that the 2 line maintenance teams start from 2 maintenance sites respectively, and each of them completes the line maintenance task according to the scheduling path solved by the line maintenance team model. Maintenance team 1 firstly departs from maintenance site 1, repairs lines L7-8, L5-6, L30-31 and L16-17 in turn, completes the maintenance of the line at t=248min, and finally returns to maintenance site 1. Maintenance team 2 firstly departs from maintenance site 2, repairs lines L3-4, L20-21 and L10-11 in turn, completes the maintenance of the line at t=180min and returns to maintenance site 2. The maintenance of the line is completed at t=180min and returned to maintenance site 2.

The two switch operation teams start from the two maintenance sites, and each of them completes the switch closing task according to the scheduling path solved by the switch operation team model. Switching team 1 starts from maintenance site 1 and reaches switches 15-16 at t = 55 min, but closes the manual switches at t = 256 min. Switch operator team 2 first departs from maintenance site 2 and closes switches 12-22, 30-31, and 18-33 sequentially, finally completing the closure of the switches at t=260min and returning to maintenance site 2.

Table 1. Scheduling paths and time

Maintenance team type	Path [Arrival time/departure time (min)]
Path team 1	7-8[15/68]→5-6[87/120]→30-31[145/195]→16-17[216/248]
Path team 2	3-4[14/66]→20-21[80/128]→10-11[155/180]
Switch team 1	15-16[55/256]
Switch team 2	12-22[45/196]→30-31[221/233]→18-33[251/260]

With the proposed multi-stage dynamic recovery model, the model continuously recovers through stages and eventually restores the loads in all microgrids throughout the system. The recovery sequence of each switch and microgrid solved by the model is shown in Table 2, and the DER (distributed energy resources) output and load recovery power's are also labeled at the corresponding time. When solving the model, the security check of the model does not have to be done in real time during the whole restoration process, but only at the moment when the load of the system changes, such as the moment t=67min (the moment when microgrid 2 completes the restoration), t=121min (the moment when microgrid 3 completes the restoration), and t=196min (the moment when microgrid 5 completes the restoration).

Table 2. Recovery sequence schedule of multi-stage dynamic recovery model

Time (min)	Switch recovery sequence	Microgrid recovery sequence	DER force (KW)	Load recovery (KW)
0		1,6,9	460	750
67	2-3	2		
68				1150
69		4	240	240
121	7-8	3		
122			150	150
129	20-21	8		
130				200
195		10	220	220
196	12-22	5		
197				175
198	9-10			
199				250
200	12-13			
233	30-31			
256	15-16	7		
257				220
260	18-33			
261				480

3.1.2. Model Superiority.The multi-stage dynamic disaster recovery model proposed in this chapter is compared with the traditional disaster recovery model to demonstrate the superiority of the proposed multi-stage dynamic disaster recovery model. The traditional recovery model also includes a line maintenance team scheduling model, a switch operation team scheduling model and a recovery model, but there is a lack of coupling constraints between the models. In the solution algorithm, the traditional recovery model first solves the line maintenance team scheduling model to obtain the maintenance time of each maintenance team, which is denoted as $A_k^{MC,RP*}$. Then, the obtained $A_k^{MC,RP*}$ is used as the input to the recovery model to solve the recovery model, which can obtain the switch closure sequence based on this maintenance time, and then obtain the movement scheduling path of the switching team, which is used as the input to the switch operation team scheduling model and is solved to obtain the operation time of the switching team. Solve to get the operation time of the switch team. It can be seen that the traditional recovery model does not consider the scheduling of the switch operation team, and solves the switch operation team scheduling model only based on the maintenance team scheduling model, which will lead to the operation time of the switch operation team not being able to be better matched, wasting the scheduling time, and prolonging the outage time. The final recovery sequence of the traditional recovery model is shown in Table 3.

From the restoration order in the table, it can be seen that the faulty lines that require short repair time will be repaired first, for example, lines L10-11 and L16-17 are repaired first, this is due to the fact that the objective function of the line maintenance team scheduling model in the traditional restoration model is to minimize the outage time of the lines, so the obtained restoration order is not the optimal restoration order. For example, lines L10-11 in microgrid 5 are repaired at moment t = 47 min, while microgrid 5 is not able to complete the load outage restoration until moment t = 257 min. Lines L16-17 in microgrid 7 are restored at moment t=175min, while microgrid 7 is not able to complete the load outage restoration until moment t=272min. The main reason is that after the line is restored, there is no corresponding distributed power supply in its microgrid, and the high-priority microgrid in its front position does not restore power supply, which leads to the corresponding switch not being able to complete the closure, delaying the load restoration timing. Comparing with the multi-stage dynamic recovery model in the previous paper, the moment of completion of recovery in the traditional recovery model (t=273min) is later than that in the multi-stage dynamic recovery model (t=261min).

Table 3. Recovery sequence schedule of traditional recovery model

Time (min)	Path maintenance	Switch recovery sequence	Microgrid recovery sequence	DER force (KW)	Load recovery (KW)
0			1,6,9	460	750
47	L10-11				
61	L20-21				
62		20-21	8		
63					200
118	L30-31				
119			10	220	220
130	L3-4				
131		2-3	2		
132				0	1200
175	L16-17				
183	L5-6				
192		4-5	3		
193					400
227		26-27			
228					220
238		30-1			
239					200
254	L7-8				
255		7-8	4		
256					240
257		9-10	5		
258					185
272		15-16	7		
273					220

3.2. *Analysis of resource movement results*

3.2.1. Analysis of results of preallocation of mobile emergency resources.The multi-stage dynamic recovery model proposed in this paper is applied and the response time limit of mobile emergency resources is set to 20 minutes. The optimal staging point locations of mobile emergency resources and their shortest traveling time to each node of the distribution network are shown in Table 4.

After comprehensively considering the risk of load outage, the cost of mobile emergency resources and other factors, it can be seen from Table 4, according to the shortest driving time between the nodes and the road resistance, we get the optimal staging point of mobile emergency resources in the distribution network area of the example of this section is node 17, and the shortest driving time from node 17 to other nodes of the distribution network are within the response time limit, which is in line with the siting requirements.

Table 4. The shortest driving time of mobile emergency resources scheduling

Node	Shortest driving time/min	Node	Shortest driving time/min	Node	Shortest driving time/min
1	18.2	12	11.6	23	11.3
2	15.1	13	13.7	24	8.5
3	12.6	14	9.6	25	6.2
4	9.3	15	5.8	26	4.2
5	11.5	16	2.4	27	5.5
6	15.7	17	0	28	8.4
7	13.6	18	2.3	29	13.7
8	14.5	19	4.9	30	11.6
9	16.4	20	6.4	31	10.5
10	13.4	21	10.6	32	8.8
11	7.1	22	9.7	33	10.5

Further, the mobile emergency resource allocation scheme of the optimal assembly point is determined. Based on the objective function of the constructed pre-allocation model, the following three schemes are set up for comparison, and the results are shown in Table 5.

Scheme 1: The objective function adopts the multi-stage dynamic recovery model of this paper, i.e., the total cost of the combined load outage loss cost, mobile emergency resources traveling fuel cost, and mobile emergency resources investment acquisition cost is minimized.

Scenario 2: The objective function considers only load outage loss cost minimization.

Scenario 3: The objective function only considers the minimization of mobile emergency resources traveling fuel costs and investment acquisition costs.

As can be seen from Table 5, Scenario 2 focuses on minimizing load outage losses by allocating as many mobile emergency resources as possible, but ignores issues such as redundancy in the allocation of mobile emergency resources and higher costs. Scheme 3 focuses on realizing the optimal cost and expense, but ignores the impact of the distribution network failure rate and load outage risk on mobile emergency resources allocation under extreme weather factors, which cannot effectively differentiate between important loads and loads with lower risk losses, and may cause differences in the selection of mobile emergency resources types and an increase in the number of configurations in the screening of important loads and allocation of restoration demand, resulting in redundancy of resource capacity.

The proposed scheme 1 in this section comprehensively considers both the risk of load outage under the influence of extreme weather and the cost of mobile emergency resource allocation, which is smaller than scheme 2 and scheme 3 in terms of the number of allocations and resource capacity, and can effectively reduce the redundancy of mobile emergency resource allocation. At the same time, since the multi-stage dynamic recovery model in this paper puts constraints on load recovery demand, it can ensure the capacity reserve of mobile emergency resources in important load recovery, which verifies the effectiveness of the multi-stage dynamic recovery model in this paper.

Table 5. Mobile emergency resources scheduling results comparison

	Assembly point	Sort 1	Sort 2	Sort 3	Sort 4	Sort 5	Total scheduling quantity
Scheme 1	Point 17	4	4	1	0	4	13
Scheme 2	Point 17	4	4	4	4	4	20
Scheme 3	Point 18	4	3	1	2	4	14

3.2.2. Analysis of mobile emergency resource mobilization results

1) Mobile emergency resources traveling path analysis. Under the time scale of 6 hours after the disaster, the mobile emergency resources of the three scenarios access the nodes in each time period, i.e., the optimization results of the driving path of mobile emergency resources. A vehicle is selected from each mobile emergency resource type as a typical case, and the scheduling optimization results obtained from the three schemes are visually compared as shown in Figure 4. Among them, the pink, green and orange lines represent the scheduling results of mobile emergency resources in Scenario 1, Scenario 2 and Scenario 3, respectively.

According to Fig. 4, it can be seen that from the 5th scheduling time cycle, the traffic network road state and distribution network line fault state will change dynamically. The scheduling scheme of each mobile emergency resource traveling path in Scenario 1 produces more obvious adjustments according to the real-time topology of the coupled power-transportation network. At the same time, as repairers repair distribution network line faults, the number of mobile emergency resources dispatched is gradually reduced according to the current load restoration demand, which is in line with the actual situation of post-disaster restoration.

Option 2 does not take into account the impact of dynamic information, mobile emergency resources traveling paths and access nodes in the entire time scale are more stable, can not effectively reflect the power-transportation coupling network post-disaster restoration status and load restoration demand and other dynamic information under the multi-temporal cross-section, there are some limitations in the engineering application level.

Scenario 3 takes into account the impact of dynamic information, and the traveling path of mobile emergency resources will be dynamically adjusted with the fault recovery process. However, Program 3 only considers load grading, and the consistent weighting of loads of the same grade makes the decision of load recovery order relatively unclear, and in the case of reducing the configuration of mobile emergency resources with dynamic information changes, the frequency of resource dispatch is relatively high compared to Program 1, which to a certain extent affects the continuity of the power supply support of the resources and increases the difficulty of scheduling, and reduces the maneuverability in the actual engineering.

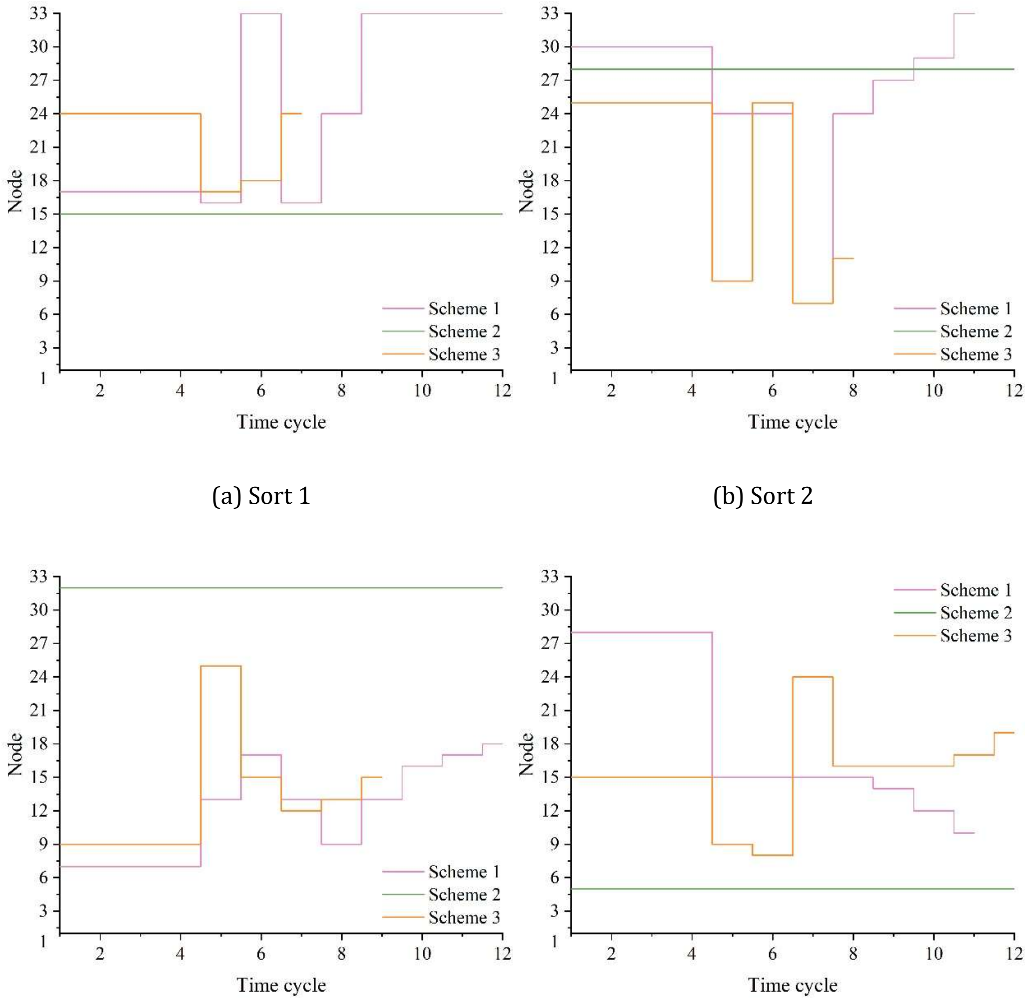

(a) Sort 1 (b) Sort 2

(c) Sort 3 (d) Sort 5

Fig. 4. Mobile emergency resources scheduling path comparison

2) Load recovery level analysis. The recovery levels of active and reactive power of important loads and loads as a whole in each time cycle, i.e., the fault recovery capability of the three schemes are shown in Figs. 5 and 6.

Since all three schemes at least consider the load weight assignment within the load grading, and take the first-level load as the important load division standard, the three schemes can reach 100% of the important load active power recovery level in each time cycle. Regarding the overall load active power recovery level, the change trend of Scenario 1 and Scenario 3 is consistent, both of which show an upward trend with the fault recovery process, fluctuating between 83.49%-88.47% in the first five dispatch time cycles and reaching 100% after the 6th-7th dispatch time cycles. Whereas, the overall active power recovery level of Scenario 2 loads fluctuates between 85.12%-88.96%. The comparison shows that Scenario 1 and Scenario 3 take into account the dynamic information changes and are able to adjust the mobile in time.

The optimization objective of mobile emergency resource scheduling is mainly to support load active power recovery, and the performance in overall reactive power recovery is relatively weak. Scenario 1 and Scenario 3 fluctuate in the range of 40%-50% in the important load reactive power recovery level and the overall load reactive power recovery level in the first 7 scheduling time cycles. In Scenario 2, the reactive power recovery level of important loads fluctuates around 25% in the first 7 dispatching time cycles, which is significantly lower than the two aforementioned scenarios, and the overall reactive power level of loads fluctuates around 40%. The important loads and the overall reactive power level of loads in Scenarios 1 and 3 gradually increase to 100%.

In summary, the resource scheduling effect of Scheme 1 using the multi-stage dynamic recovery model of this paper is the best.

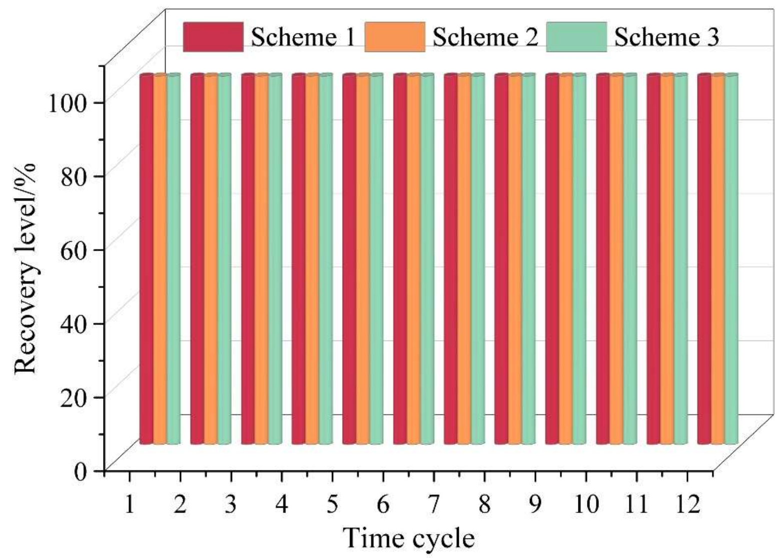

(a) Important load power recovery level

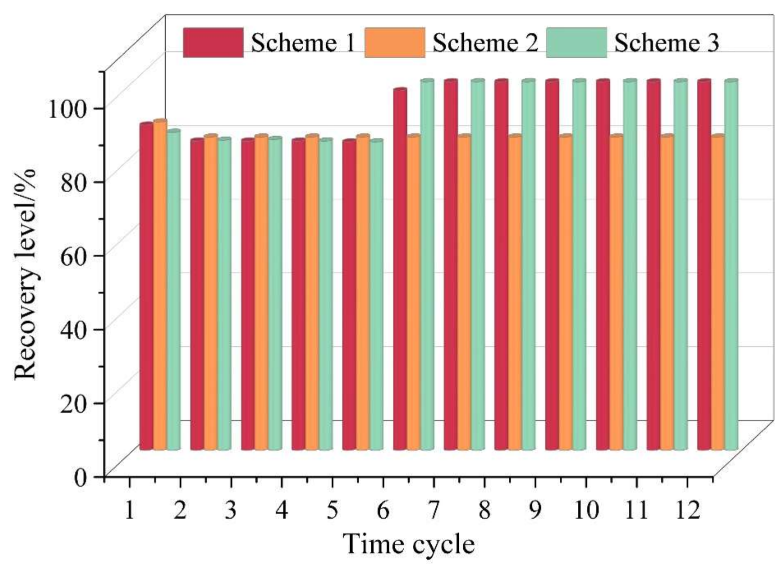

(b) Load overall power recovery level

Figure 5 Load power recovery level

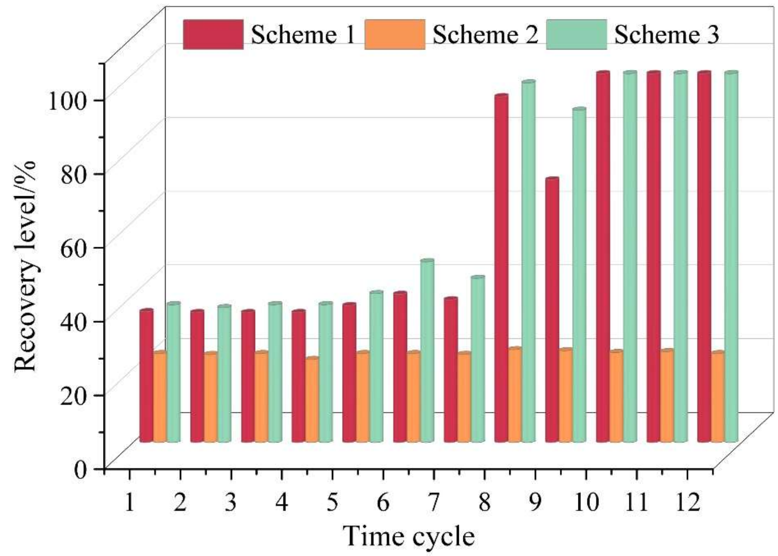

(a) Important load reactive power recovery level

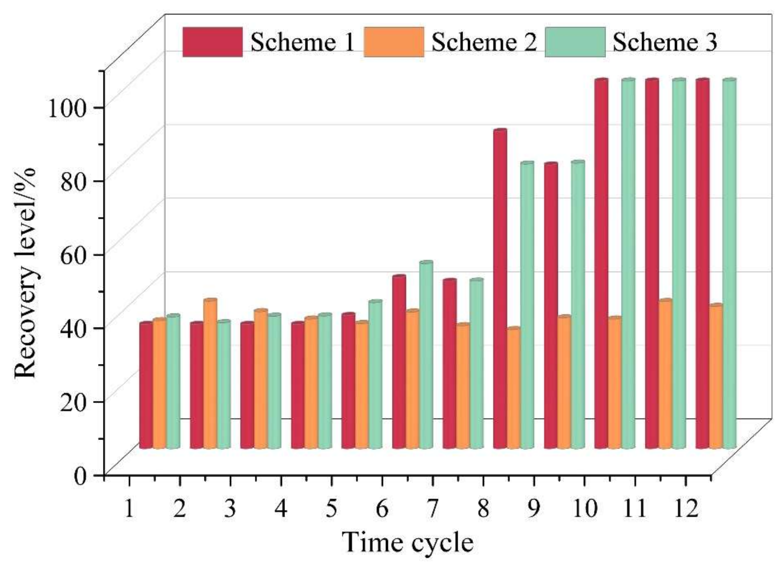

(b) Load overall reactive power recovery level

Fig. 6. Load reactive power recovery level

4. Conclusion

In this paper, a multi-stage dynamic resilient recovery strategy with multiple energy storage is adopted for phased recovery planning of urban distribution networks after a disaster. The typhoon disaster is taken as an example to optimize the post-disaster defense measures in coastal cities based on the recovery strategy. The multi-stage dynamic recovery model proposed in this paper is tested for its post-disaster recovery and resource scheduling effects through an

arithmetic example analysis.
1) In the example analysis, it takes 261 minutes to complete the restoration of this paper's multi-stage dynamic recovery model, while the traditional recovery model takes 273 minutes, and this paper's multi-stage dynamic recovery model has a better post-disaster recovery effect.
2) The number of vehicles used in the dispatching scheme proposed by this paper's multi-stage dynamic recovery model is the smallest among all dispatching schemes (13 vehicles), which effectively saves resource capacity. And the traveling path of mobile emergency resources of this scheme is most consistent with the situation of post-disaster restoration. This paper's scheme has the best load reactive power and active power restoration levels. In the first 5 scheduling time cycles, the active power fluctuates between 83.49%-88.47% and reaches 100% after the 6th-7th scheduling time cycles. The reactive power recovery level fluctuates between 40%-50% during the first 7 scheduling time cycles and is 100% after 10-12 scheduling time cycles.

Funding

This research was supported by the Science and Technology Project of China Southern Power Grid Company Limited (Project No. 090000KKK52222158).

References

[1] Chen, C., Wang, J., & Ton, D. (2017). Modernizing distribution system restoration to achieve grid resiliency against extreme weather events: An integrated solution. Proceedings of the IEEE, 105(7), 1267-1288.

[2] Arif, A., Wang, Z., Wang, J., & Chen, C. (2017). Power distribution system outage management with co-optimization of repairs, reconfiguration, and DG dispatch. IEEE Transactions on Smart Grid, 9(5), 4109-4118.

[3] Lei, S., Chen, C., Li, Y., & Hou, Y. (2019). Resilient disaster recovery logistics of distribution systems: Co-optimize service restoration with repair crew and mobile power source dispatch. IEEE Transactions on Smart Grid, 10(6), 6187-6202.

[4] Nazemi, M., Moeini-Aghtaie, M., Fotuhi-Firuzabad, M., & Dehghanian, P. (2019). Energy storage planning for enhanced resilience of power distribution networks against earthquakes. IEEE Transactions on Sustainable Energy, 11(2), 795-806.

[5] Huang, G., Wang, J., Chen, C., Qi, J., & Guo, C. (2017). Integration of preventive and emergency responses for power grid resilience enhancement. IEEE Transactions on Power Systems, 32(6), 4451-4463.

[6] Huang, Q., Huang, R., Hao, W., Tan, J., Fan, R., & Huang, Z. (2019). Adaptive power system emergency control using deep reinforcement learning. IEEE Transactions on Smart Grid, 11(2), 1171-1182.

[7] Poudel, S., & Dubey, A. (2018). Critical load restoration using distributed energy resources for resilient power distribution system. IEEE Transactions on Power Systems, 34(1), 52-63.

[8] Panteli, M., Trakas, D. N., Mancarella, P., & Hatziargyriou, N. D. (2017). Power systems resilience

assessment: Hardening and smart operational enhancement strategies. Proceedings of the IEEE, 105(7), 1202-1213.

[9] Román, M. O., Stokes, E. C., Shrestha, R., Wang, Z., Schultz, L., Carlo, E. A. S., ... & Enenkel, M. (2019). Satellite-based assessment of electricity restoration efforts in Puerto Rico after Hurricane Maria. PloS one, 14(6), e0218883.

[10] Chen, B., Chen, C., Wang, J., & Butler-Purry, K. L. (2017). Multi-time step service restoration for advanced distribution systems and microgrids. IEEE Transactions on Smart Grid, 9(6), 6793-6805.

[11] Bie, Z., Lin, Y., Li, G., & Li, F. (2017). Battling the extreme: A study on the power system resilience. Proceedings of the IEEE, 105(7), 1253-1266.

[12] Li, Z., Shahidehpour, M., Aminifar, F., Alabdulwahab, A., & Al-Turki, Y. (2017). Networked microgrids for enhancing the power system resilience. Proceedings of the IEEE, 105(7), 1289-1310.

[13] Jufri, F. H., Widiputra, V., & Jung, J. (2019). State-of-the-art review on power grid resilience to extreme weather events: Definitions, frameworks, quantitative assessment methodologies, and enhancement strategies. Applied energy, 239, 1049-1065.

[14] Ding, T., Wang, Z., Jia, W., Chen, B., Chen, C., & Shahidehpour, M. (2020). Multiperiod distribution system restoration with routing repair crews, mobile electric vehicles, and soft-open-point networked microgrids. IEEE Transactions on Smart Grid, 11(6), 4795-4808.

[15] Shao, C., Shahidehpour, M., Wang, X., Wang, X., & Wang, B. (2017). Integrated planning of electricity and natural gas transportation systems for enhancing the power grid resilience. IEEE Transactions on Power Systems, 32(6), 4418-4429.

[16] Klein, N. (2018). The battle for paradise: Puerto Rico takes on the disaster capitalists. Haymarket Books.

[17] He, C., Dai, C., Wu, L., & Liu, T. (2018). Robust network hardening strategy for enhancing resilience of integrated electricity and natural gas distribution systems against natural disasters. IEEE Transactions on Power Systems, 33(5), 5787-5798.

[18] Gholami, A., Shekari, T., Amirioun, M. H., Aminifar, F., Amini, M. H., & Sargolzaei, A. (2018). Toward a consensus on the definition and taxonomy of power system resilience. IEEE Access, 6, 32035-32053.

[19] Bhusal, N., Abdelmalak, M., Kamruzzaman, M., & Benidris, M. (2020). Power system resilience: Current practices, challenges, and future directions. Ieee Access, 8, 18064-18086.

[20] Ding, T., Lin, Y., Bie, Z., & Chen, C. (2017). A resilient microgrid formation strategy for load restoration considering master-slave distributed generators and topology reconfiguration. Applied energy, 199, 205-216.

[21] Mahzarnia, M., Moghaddam, M. P., Baboli, P. T., & Siano, P. (2020). A review of the measures to enhance power systems resilience. IEEE Systems Journal, 14(3), 4059-4070.

[22] Zhang, W., Wang, N., & Nicholson, C. (2017). Resilience-based post-disaster recovery strategies for road-bridge networks. Structure and Infrastructure Engineering, 13(11), 1404-1413.

[23] Inneke Van Hoeck & Pieter Vansteenwegen. (2024). A MILP model to improve the robustness of a railway timetable by retiming and rerouting in a complex bottleneck area. Journal of Rail

Transport Planning & Management100488-100488.

[24] Christina Lee Min Eh,Angnes Ngieng Tze Tiong,Chun Hsion Lim,Jibrail Kansedo,Bing Shen How & Wendy Pei Qin Ng. (2024). A MILP model for integrated circular hydrogen economy based in Malaysia with intermodal transportation. International Journal of Hydrogen Energy1320-1334.

[25] Wang Lina,Wang Hejing,Yang Xin,Gao Yanfeng,Cui Xiaohong & Wang Binrui. (2022). Research on smooth path planning method based on improved ant colony algorithm optimized by Floyd algorithm. Frontiers in Neurorobotics955179-955179.